CrossMark

ORIGINAL

In-vivo and In-vitro Metabolism Study of Timosaponin B-II Using HPLC-ESI-MS^{n}

Yao Jia[1,2] · Zhiwen Fu[1,3] · Zhixiong Li[1] · Pei Hu[1] · Rui Xue[1] · Mingcang Chen[1] · Ting Xiang[2] · Chenggang Huang[1]

Abstract Timosaponin B-II (TB-II), a representative furostanol saponin in *Rhizoma anemarrhenae*, has been used as an emperor herb in many Chinese herbal formulas to treat diabetes and senile dementia. However, its metabolism and tissue distribution had not been investigated so far. In this work, a sensitive and specific high-performance liquid chromatography-electrospray ionization tandem mass spectrometry method was applied for the identification of TB-II and its major metabolites in in-vivo and in-vitro samples. Rat urine, feces, plasma and tissues were collected after oral administration of TB-II at a single dose of 300 mg kg^{-1}. Furthermore, TB-II was incubated in artificial gastric juice (AGJ) and artificial intestinal juice (AIJ). As a result, 19 metabolites were detected and identified by comparing their HPLC behavior and MS^{n} spectra profile with those of the parent drug. Moreover, the structures of its five metabolites were identified by using the standards prepared by the acid hydrolysis of TB-II. In addition to the parent drug, 14, 12, 6, 1, 1 and 7 metabolites were detected in rat urine, feces, plasma, heart, kidney and liver, respectively, while no metabolites or the parent drug were found in rat brain, spleen and lung. Seven metabolites appeared in AIJ incubation samples, but the parent drug was absent. Nine metabolites along with the parent drug were observed in AGJ incubation samples. The biotransformation pathways of TB-II mainly included dehydration, deglycosylation, hydroxylation, oxidation and E-ring cleavage. This is the first comprehensive investigation of the in-vivo and in-vitro metabolism of TB-II. The result provided important information for further pharmacological research on TB-II.

Keywords HPLC-ESI-MS^{n} · Timosaponin B-II · Metabolism · Tissue distribution

Y. Jia and Z. Fu contributed equally to the work.

✉ Ting Xiang
  tingxiang39@163.com

✉ Chenggang Huang
  cghsimm@126.com

1 Shanghai Institute of Materia Medica, Chinese Academy of Sciences, 501 Haike Rd., ZhangJiang, Pudong, Shanghai 201203, People's Republic of China

2 Institute of Pharmaceutical Research, Yangtze River Pharmaceutical Group, 16 Shengming Yuan Road, Changpiing, Beijing 102206, People's Republic of China

3 Shanghai University of Traditional Chinese Medicine, Shanghai, People's Republic of China

Introduction

Timosaponin B-II (TB-II), (25*S*)-26-*O*-β-D-glucopyranosyl-22-hydroxy-5β-furostane-3β,26-diol-3-*O*-β-D-glucopyranosyl-(1 → 2)-β-D-galactopyranoside [1, 2] (Fig. 1) was reported as the major furostanol saponin in *Rhizoma anemarrhenae*. In our previous studies [3, 4], TB-II could be found in rat serum and urine after oral administration of Huangbai-Zhimu herb-pair extract and a *Rhizoma anemarrhenae* decoction, respectively. According to the theories of serum pharmacochemistry, TB-II was the key efficacy component of *Rhizoma anemarrhenae*. Recent pharmacological research showed that TB-II could significantly inhibit platelet aggregation and thrombus formation [5, 6], the expression of proinflammatory cytokines [7] and the proliferation of vascular smooth muscle cells [8]. Moreover, TB-II could improve memory and learning deficits and have an anti-dementia effect [9], protect primary neurons against Aβ$_{25–35}$ induced toxicity [10], potentiate the brain 5-HT and DA nerve systems and act as an antidepressant [11]. However, it was poorly absorbed

Fig. 1 The chemical structure
of TB-II

Timosaponin B-II

$C_{45}H_{76}O_{19}$
Exact Mass: 920.4981
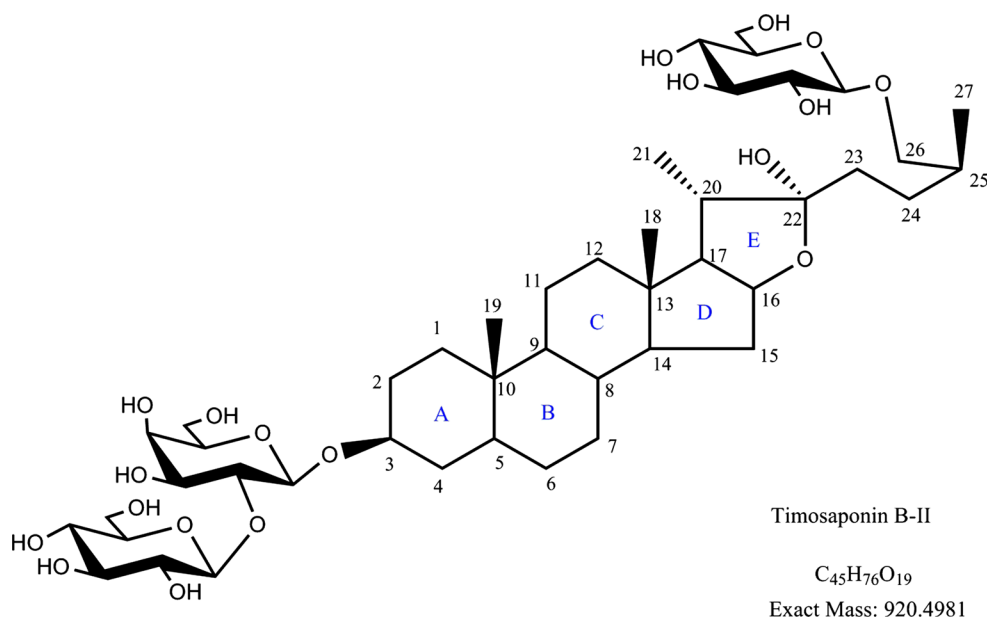
via the gastrointestinal segment or may have undergone acid-induced degradation following oral administration to rats, with the absolute oral bioavailability being only 1.1 ± 0.3 % [12, 13]. It could be inferred that the metabolites of TB-II might be the authentic effective factors rather than the parent compound.

Against this background, an investigation of the metabolism of TB-II is of great significance for the elucidation of its pharmacological mechanisms and even the development of novel drugs from its metabolites. Liu et al. [14, 15] compared the pharmacokinetics of timosaponin B-II in rat plasma after oral administration of Zhimu-Baihe herb-pair, Zhimu extract and free timosaponin B-II; moreover, they studied the metabolites of *Anemarrhena asphodeloides* saponin extract. Feng et al. [16] also performed the determination of TB-II in rat plasma and carried out a pharmacokinetic study. However, there have been no reports on a comprehensive in-vivo and in-vitro metabolism study of TB-II.

In the present study, a sensitive and specific HPLC-ESI-MS^n method was used for systematic analysis and identification of TB-II and its 19 metabolites in biological samples of in-vivo rat experiments and in-vitro incubation experiments. In addition, the structures of its seven metabolites were unambiguously identified by using the prepared standards together with the previously isolated standards of timosaponin B-III (TB-III) and timosaponin A-III (TA-III), while the others were tentatively identified by comparing their HPLC behavior and MS^n spectra profile with those of the parent drug (TB-II). The results of this study will be helpful for better understanding the metabolic processes of TB-II and the potential pharmacological application of these metabolites.

Experimental

Materials and Reagents

TB-II, TB-III and TA-III (purities >98 %) were isolated and purified from *Rhizoma anemarrhenae*. Five artificial steroidal saponins (timosaponin BII-b, timosaponin BII-d, timosaponin BIII-a, timosaponin BIII-b and timosaponin BIII-c) were obtained previously by our laboratory [17, 18]. Their structures (Fig. 2) were confirmed by ^{1}H-NMR, ^{13}C-NMR, 2D NMR and MS and compared with the literature. Pepsin (1:15,000, CAT: 88918B) and pancreatin (USP, CAT: 84278A) were purchased from Adamas Reagent Co., Ltd. (Shanghai, China). Acetonitrile and formic acid were HPLC grade from Fisher Scientific (Tustin, CA, USA). Water was triple distilled using a Milli-Q system (Millipore, Billerica, MA, USA). All other analytical grade reagents were purchased from Sinopharm Chemical Reagent Co., Ltd. (Shanghai, China). Pretreatment of samples by SPE was performed with Waters Oasis HLB cartridges (30 mg, 1 mL) obtained from Waters (Milford, MA, USA).

Chromatographic System and Mass Spectrometry Conditions

The chromatographic separations were performed using a reversed-phase column (Inertsil ODS-3, 4.6 mm × 250 mm i.d., 5 µm, GL Science, Tokyo, Japan) connected to an Easy-Guard Kit C18 (4 mm × 2 mm, Grace, USA) guard column, with the column temperature set at 25 °C. The mobile phase consisted of linear gradients of 0.1 % (v/v) ammonia (A) and acetonitrile (B): 0–10 min, 10–27 % B (v/v); 10–18 min, 27–29 % B; 18–40 min, 29–95 % B.
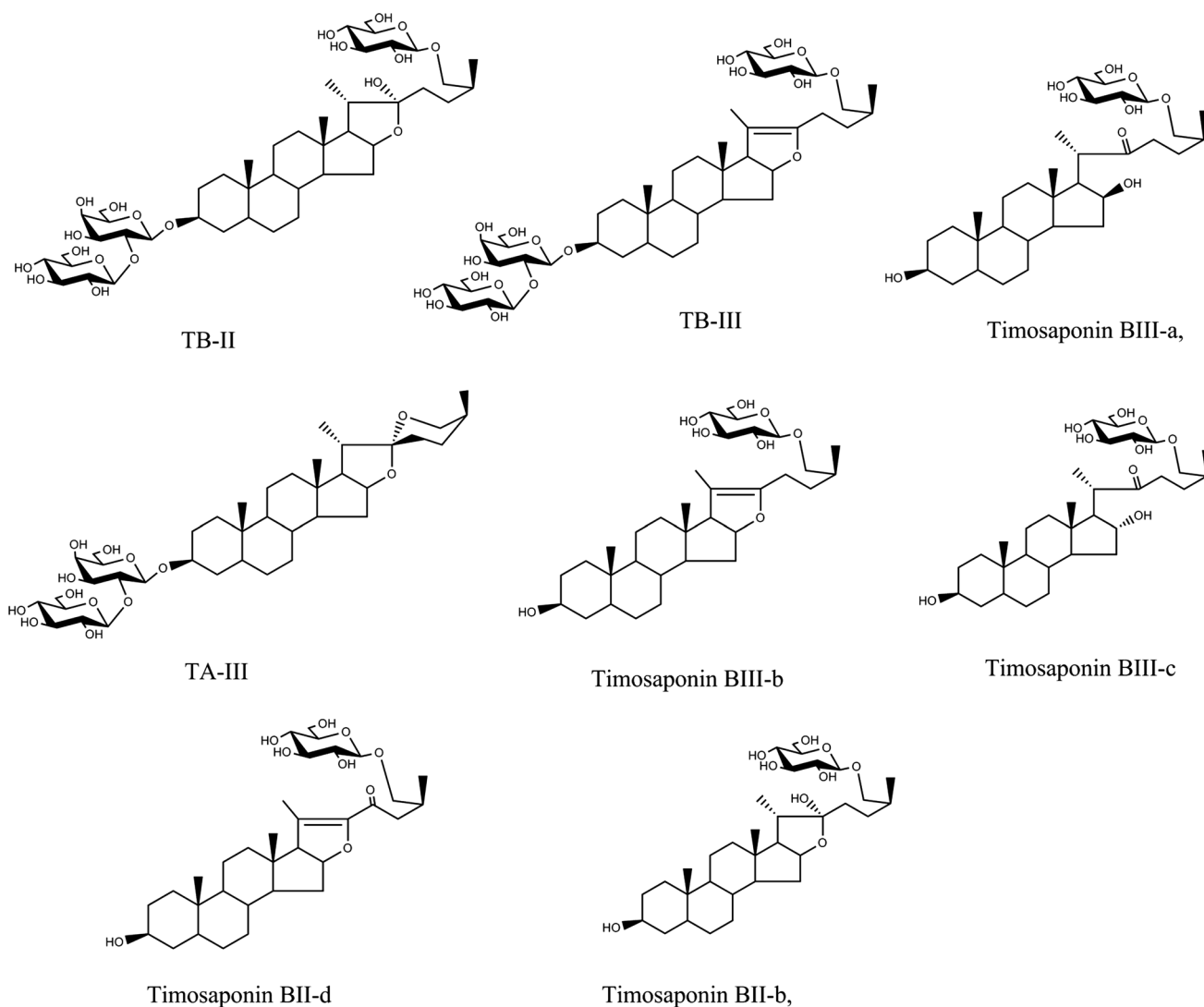
Fig. 2 Structures of eight reference compounds

The composition was then held at 95 % B for 5 min. Then the gradients were returned to 10 % B and maintained for 10 min for equilibration. The mobile phase flow rate was 1.0 mL·min^{-1}, and the whole analysis time was 55 min.

The LC-MS^n analysis was performed on a 1200 Series HPLC instrument (Agilent, Waldbronn, Germany) coupled with a 6300 Series ion trap (IT) (Agilent Technology, Palo Alto, CA, USA) via an electrospray ionization (ESI) interface. The hardware inclued an Agilent 1200 Series LC and the 6300 series ion trap mass spectrometer. The software (version 6.1) included the Trap Control Program for trap control, data acquisition, data analysis, quantitative analysis and the LC control programs. MS^n analyses were conducted in negative-ion mode, and the instrument was operated under the following optimized conditions: collision gas, ultra-high-purity helium (He); nebulizing gas, high-purity nitrogen (N$_2$); capillary voltage, 3.5 kV; end

plate offset, 500 V; nebulizer, 30 psi; drying gas flow rate, 10 L·mL^{-1}; drying gas temperature, 350 °C. For full-scan MS analysis, the spectra were recorded in the range of m/z 50–1500.

Animals and Drug Administration

Twenty-six male Sprague-Dawley rats (200–220 g) were supplied by Shanghai SLAC Laboratory Animal Co., Ltd. (Shanghai, China). All animal experiments adhered to protocols approved by the Review Committee of Animal Care and Use at the Shanghai Institute of Materia Medica (Shanghai, China). The animals were divided into three groups at random: group A for dosed urine and feces collection ($n = 2$); group B for dosed blood and tissue withdrawal ($n = 20$); group C for blank urine and feces, blood and tissue collection ($n = 4$). Animals were fasted

overnight, but with access to water, and administered TB-II by oral gavage at a single dose of 300 mg kg^{-1}.

Sample Preparation

In-vivo Samples

Urine samples were collected from 0 to 24 h after administration and centrifuged at $10,000 \times g$ for 10 min. Feces samples were collected from 0 to 24 h after the dose, dried for 48 h at 37 °C and crushed. Blood samples were withdrawn from the abdominal aorta in heparinized tubes at 0.5, 1.0, 1.5, 2.0, 3.0, 4.0, 6.0, 8.0, 10.0 and 12.0 h after administration of TB-II (with two rats at each time point) and centrifuged at $4000 \times g$ for 10 min to obtain the plasma. Tissues, including brain, heart, liver, spleen, lung and kidney, were obtained at 2.0, 4.0, 6.0, 8.0, 10.0 and 12.0 h after the treatment of TB-II (with two rats at each time point), then weighed, homogenized with 0.1 M PBS buffer (pH 7.4) at a ratio of 1 g/5 mL and centrifuged at $10,000 \times g$ for 20 min to obtain the supernatants. Then 400 μL urine, plasma and tissue homogenates obtained from each time point were combined as the drug-containing plasma, urine and tissue homogenate samples, respectively. All samples were stored at −80 °C until they were analyzed.

The drug-containing sample (600 μL) was loaded onto a SPE cartridge that was preconditioned with 1 mL methanol and 1 mL water subsequently. The cartridge was then washed with 1 mL water and the analytes were eluted with 1 mL methanol, respectively. The 200-mg crushed feces sample was extracted by ultrasonication three times with 5 mL acetonitrile-water (1:1, v/v) for 30 min each time. The extracted solutions, with the different pretreatment methods described above, were all dried under nitrogen gas over a 37 °C water bath. The residues were then dissolved with 200 μL acetonitrile-water (1:1, v/v) and centrifuged at $10,000 \times g$ for 10 min at 4 °C. The supernatant was analyzed by LC–MS-MS. Blank samples as controls were prepared with the same method as for the drug-containing samples.

In-vitro Samples

The AGJ and AIJ were prepared as described in the literature [19]. Samples of 30 μL TB-II (20 mg mL^{-1}) were added separately to 3-mL volumes of AGJ and AIJ and incubated in a water-bathing vibrator at 37 °C. After 0, 0.5, 1.0, 2.0, 4.0, 8.0 and 12.0 h in AGJ, and 0, 1.0, 2.0, 4.0, 8.0, 12.0 and 24.0 h in AIJ (with two samples at each time point), reactions were terminated by adding 3 mL acetonitrile. Blank samples were terminated after 12.0 h in AGJ and 24.0 h in AIJ. All sample preparations were in accordance with the procedures described for in-vivo samples.

Results and Discussion

Optimization of MS Ion Modes and LC Mobile Phase Additives

Choosing an appropriate ion mode would be more conducive to detecting and characterizing the analytes from biological samples; both the positive and negative ion modes were thus tested using TB-II. For the positive ion mode, the ion at m/z 903.6 ($[M-H_2O + H]^+$) was obtained as the quasi-molecular ion peak in the primary mass spectra (Fig. 3c), which was possibly produced by loss of the hydroxyl at the C-22 position. It was similar to the quasi-molecular ion peak of timosaponin B-III and would be prone to cause confusion if this quasi-molecular ion were used to speculate the molecular formula. Therefore, the negative ion mode was selected as the mass scan ion mode.

Furthermore, the additives in mobile phases also needed to be examined. A suitable additive added to the mobile phases could alleviate the peak tailing and increase the ionization effect. As can be seen in Fig. 3a, b, the ions at m/z 955.4 ($[M + HCOOH-H]^-$) and m/z 919.5 ($[M-H]^-$) were simultaneously obtained when 0.2 % formic acid was used as
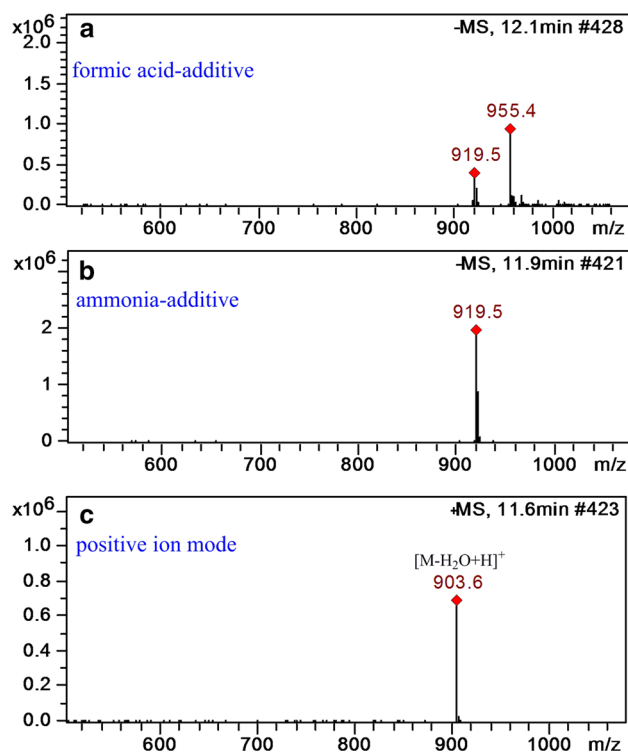
Fig. 3 ESI(-) MS spectra of TB-II during optimization: **a** with 0.2 % formic acid as additive in negative ion mode; **b** with 0.1 % ammonia as additive in negative ion mode; **c** with 0.2 % formic acid as additive in positive ion mode

the additive, while only one ion at m/z 919.5 ([M-H]$^-$) was acquired for 0.1 % ammonia. Moreover, the latter abundance of the quasi-molecular ion peak was higher because the stronger ability of ammonia to achieve protons which had a benefit for the formation of [M-H]$^-$. The formation of [M + HCOO]$^-$ would impede the potential of the multiple-stage fragmentation technique. Therefore, 0.1 % ammonia was used as the additive.

Metabolism of TB-II In Vivo

In order to identify the metabolites of TB-II, probable structures were first speculated according to the metabolism rule of drugs in vivo. The full-scan mass spectra of the free fractions obtained from dosed rat plasma, urine, feces and six selected tissues were compared with those of blank rat biological samples and the drug standard solution to explore the possible metabolites. Identification and structural elucidation of these metabolites were performed by comparing their changes in molecular masses (ΔM), retention times and mass spectral patterns of product ions with those of the parent drug. Using the negative ion mode, the parent compound and 18 metabolites were detected in rat plasma, urine, feces and six selected tissues. Extracted ion chromatographic peaks of these metabolites are shown in Fig. 4. The location and MS^n data along with the retention times of TB-II and its metabolites are summarized in Table 1. Our results indicated that dehydration, deglycosylation, oxidation and E-ring cleavage were the major metabolic pathways of TB-II in vivo.

Characterization of Metabolites in Rat Plasma and Feces

Parent Compound (M0)

Since it has been well proven by LC–MS analysis that the parent compounds and their metabolites always have very similar chemical structures, the structures of metabolites can be rapidly characterized by comparing their product ions with those of the parent drug, even if no standard substance is available for each metabolite [20]. Therefore, in order to identify metabolites of TB-II, it is first necessary to analyze the regular fragmentation patterns of TB-II. The standard TB-II was detected at 11.9 min and gave the precursor ion of [M-H]$^-$ at m/z 919, which was the base peak in the ESI mass spectrum (negative ion mode). Additionally, the MS^2 spectrum of the ion at m/z 919 gave the product ion at m/z 757 [M-C$_6$H$_{10}$O$_5$-H]$^-$, the MS^3 spectrum of the ion at m/z 757 from the m/z 919 ion yielded the m/z 595 [M-2 × C$_6$H$_{10}$O$_5$-H]$^-$ ion, and the MS^4 spectrum of the ion at m/z 595 from the m/z 757 ion produced the m/z 433 [M-3 × C$_6$H$_{10}$O$_5$-H]$^-$ ion (Fig. 5a–d). These characteristic

product ions of TB-II were the most important information for the identification of its metabolites [3, 4]. The retention time and MS^n spectra of the molecular ion at m/z 919 (M0) were consistent with those of the authentic standard. Therefore, M0 could be confirmed as the unchanged parent drug.

Dehydration Metabolite (M1)

M1 with the retention time of 15.6 min gave the [M-H]$^-$ ion at m/z 901, which was 18 Da less than that of the parent drug. There would be one dehydration reaction existing at TB-II. In addition, the characteristic fragment ions of M1 in the MS^2, MS^3 and MS^4 spectrum were at m/z 739 [M-C$_6$H$_{10}$O$_5$-H]$^-$, 577 [M-2 × C$_6$H$_{10}$O$_5$-H]$^-$ and 415 [M-3 × C$_6$H$_{10}$O$_5$-H]$^-$, respectively. Compared with the standard compound of TB-III, M1 could be confirmed as TB-III.

Deglycosylated Metabolites (M4, M5, M17 and M19)

M4 and M5 showed the [M-H]$^-$ ion at m/z 757 in the MS^2 spectrum, which was 162 Da less than that of M0. The product ion at m/z 595 [M-C$_6$H$_{10}$O$_5$-H]$^-$ could be observed in the MS^2 spectrum, which consecutively caused the deglycosylated fragment ions at m/z 433 in the MS^3 spectrum. According to the fragmentation pathways obtained above, M4 and M5 were tentatively identified as the deglycosylataed metabolites of TB-II. The sites of metabolism might be the branched chain glucose at C-3 or C-26. As for the other two deglycosylated metabolites (M17 and M19), which were consistent with those of the authentic standards, they could be directly identified as TB-II-b and TB-III-b.

Deglycosylated and Dehydration Metabolite (M9)

M9, which was detected at 26.8 min, afforded the [M-H]$^-$ ion at m/z 739, which was decreased by 180 Da compared to that of M0 and sequentially fragmented in the same pathway as M0. With the aid of the standard, M9 was identified as timosaponin AIII. It could be inferred that M9 was produced from the C-26 deglycosylated metabolite (M4/M5) by the loss of a molecule of H$_2$O and further formed spirostan saponin through the cyclization of the F ring.

Hydroxylation Metabolites (M2, M3, M6–M8 and M10–M12)

M2 and M3 were eluted at 10.0 min and 10.9 min, respectively, which were both shorter than that of TB-II. The [M-H]$^-$ ion at m/z 935 successively yielded the product ions at m/z 773 [M-C$_6$H$_{10}$O$_5$-H]$^-$, 611 [M-2 × C$_6$H$_{10}$O$_5$-H]$^-$ and

Fig. 4 Extracted ion chromatograms (EIC) of TB-II and its metabolites
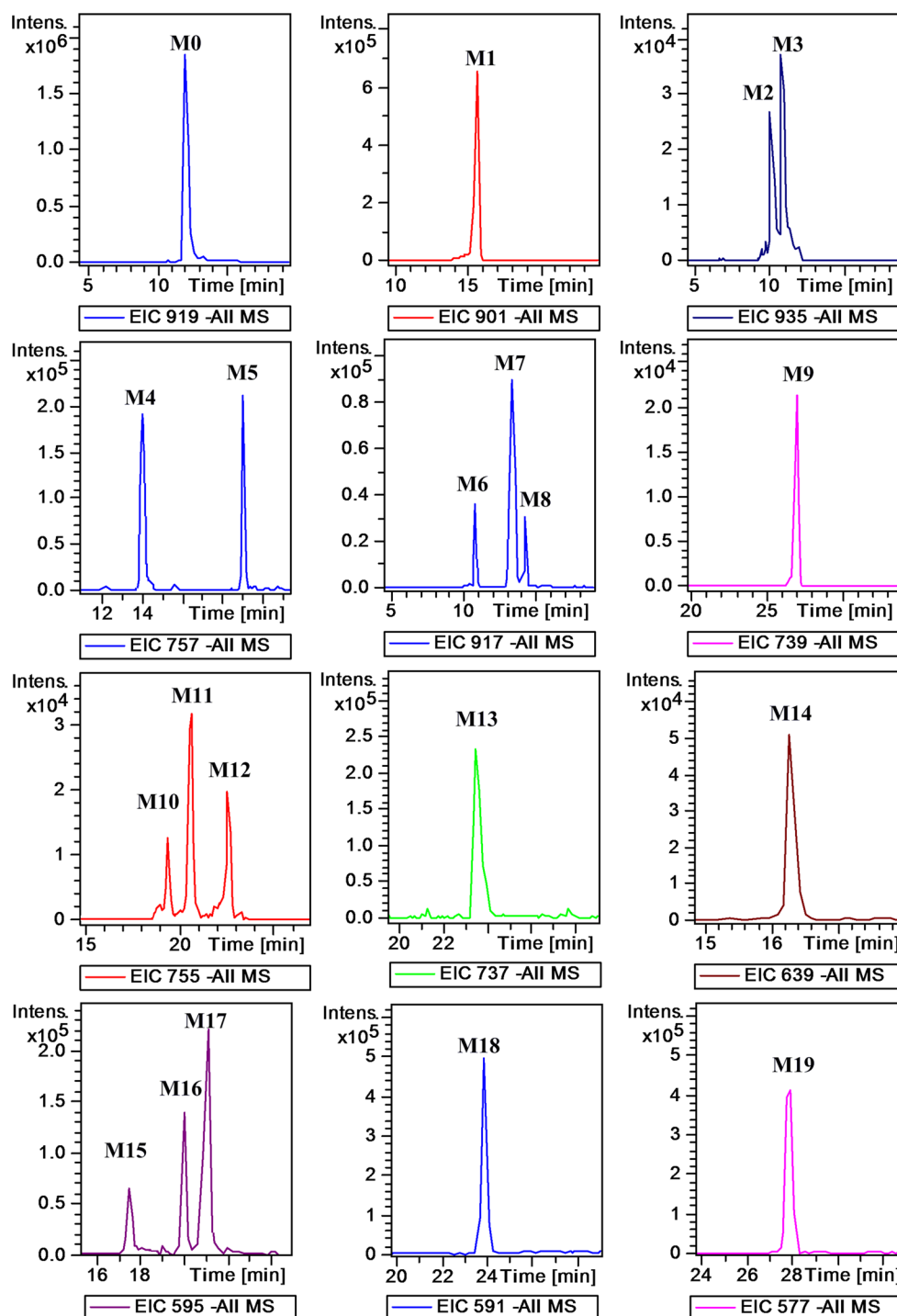
449 [M-3 × $C_6H_{10}O_5$-H]$^-$ in the MS^n spectra of **M2** and **M3**, which were all 16 Da higher than those of the parent drug. The above fragments indicated that **M2** and **M3** should be the hydroxylation metabolites of timosaponin B-II.

As for the metabolites of **M6**, **M7** and **M8**, they coexisted in the extracted ion chromatograms of m/z 917, which were eluted at 11.3 min, 13.2 min and 14.1 min, respectively. Series of characteristic product ions [M-$C_6H_{10}O_5$-H]$^-$ at m/z

755, [M-2 × $C_6H_{10}O_5$-H]$^-$ at m/z 593 and [M-3 × $C_6H_{10}O_5$-H]$^-$ at m/z 431 could be found in the MS^n spectra. Moreover, these three metabolites were eluted earlier than **M1** (TB-III) on chromatographic columns. The above observations provided clear evidence that **M6**, **M7** and **M8** might be the hydroxylation metabolites of timosaponin B-III. Similarly, the other three isomers of **M10**, **M11** and **M12** (t_R = 19.4 min, 20.5 min, 22.5 min, respectively), with the

**Table 1** Chromatographic retention time, location and MS^n data of timosaponin B-II and its metabolites

No.	t_R (min)	Distribution											[M-H]⁻	ESI-MS^n data (m/z)
		1	2	3	4	5	6	7	8	9	10	11		
M0	11.9	−	+	+	+	−	−	+	+	+	−	+	919	MS^2[919]: 757, 595 MS^3[757]: 595, 433 MS^4[595]: 433, 475
M1	15.6	−	+	−	−	−	−	−	+	+	+	+	901	MS^2[901]: 739, 577 MS^3[739]: 577 MS^4[577]: 415, 485,
M2	10.0	−	+	−	−	−	−	−	+	+	−	−	935	MS^2[935]: 773, 917, 611 MS^3[773]: 611, 449, 755 MS^4[611]: 449
M3	10.9	−	+	−	−	−	−	−	+	+	−	−	935	MS^2[935]: 773, 611, 499 MS^3[773]: 611, 499, 755
M4	14.0	−	−	−	+	−	−	−	+	+	−	−	757	MS^2[757]: 595, 577, 433 MS^3[595]: 433, 415, 475
M5	18.8	−	−	−	+	−	−	−	+	+	−	+	757	MS^2[757]: 595 MS^3[595]: 433, 575
M6	11.3	−	+	−	−	−	−	−	−	+	−	−	917	MS^2[917]: 755, 593 MS^3[755]: 593 MS^4[593]: 431
M7	13.2	−	+	−	−	−	−	−	+	+	−	+	917	MS^2[917]: 755, 593 MS^3[755]: 593 MS^4[593]: 431, 474
M8	14.1	−	+	−	−	−	−	−	+	+	−	−	917	MS^2[917]: 755, 593 MS^3[755]: 593 MS^4[593]: 431
M9	26.8	−	−	+	+	−	−	+	+	+	+	+	739	MS^2[739]: 577 MS^3[577]: 415
M10	19.4	−	−	−	+	−	−	−	−	+	−	+	755	MS^2[755]: 593 MS^3[593]: 431, 413, 473
M11	20.5	−	−	−	+	−	−	−	−	+	−	+	755	MS^2[755]: 593 MS^3[593]: 431, 485
M12	22.5	−	−	−	+	−	−	−	−	+	−	+	755	MS^2[755]: 593 MS^3[593]: 431, 575
M13	23.7	−	−	−	+	−	−	−	−	−	−	−	737	MS^2[737]: 575 MS^3[575]: 413, 161, 455
M14	16.5	−	−	−	−	−	−	−	+	+	+	+	639	MS^2[639]: 477 MS^3[477]: 459, 161
M15	17.6	−	−	−	−	−	−	−	−	−	+	−	595	MS^2[595]: 433 MS^3[433]: 415, 289
M16	20.0	−	−	−	−	−	−	−	−	−	+	−	595	MS^2[595]: 433 MS^3[433]: 415, 289, 315
M17	21.0	−	−	−	−	−	−	−	+	+	+	+	595	MS^2[595]: 433 MS^3[433]: 415, 289
M18	23.8	−	−	−	−	−	−	−	+	−	−	−	591	MS^2[591]: 429 MS^3[429]: 411
M19	27.7	−	−	−	−	−	−	−	+	−	+	−	577	MS^2[577]: 415, 485 MS^3[415]: 397, 161

1, Brain; 2, plasma; 3, heart; 4, liver; 5, spleen; 6, lung; 7, kidneys; 8, feces; 9, urine; 10, artificial intestinal juice incubation; 11, artificial gastric juice incubation; +, found; −, not found

same parent ions at m/z 755, could be temporarily identified as the hydroxylation metabolites of timosaponin A-III.

However, because of the limitation of mass spectra, we can only speculate about the possible structure of the metabolites or the relationship between metabolites and parent compounds. On this occasion, the position of hydroxy groups of **M2**, **M3**, **M6–M8 and M10–M12** could not be assigned exactly. As reported in the previous papers, C_2 and C_{15} may be prone to hydroxylation, and they were the most possible metabolism sites [14, 21, 22]. However,
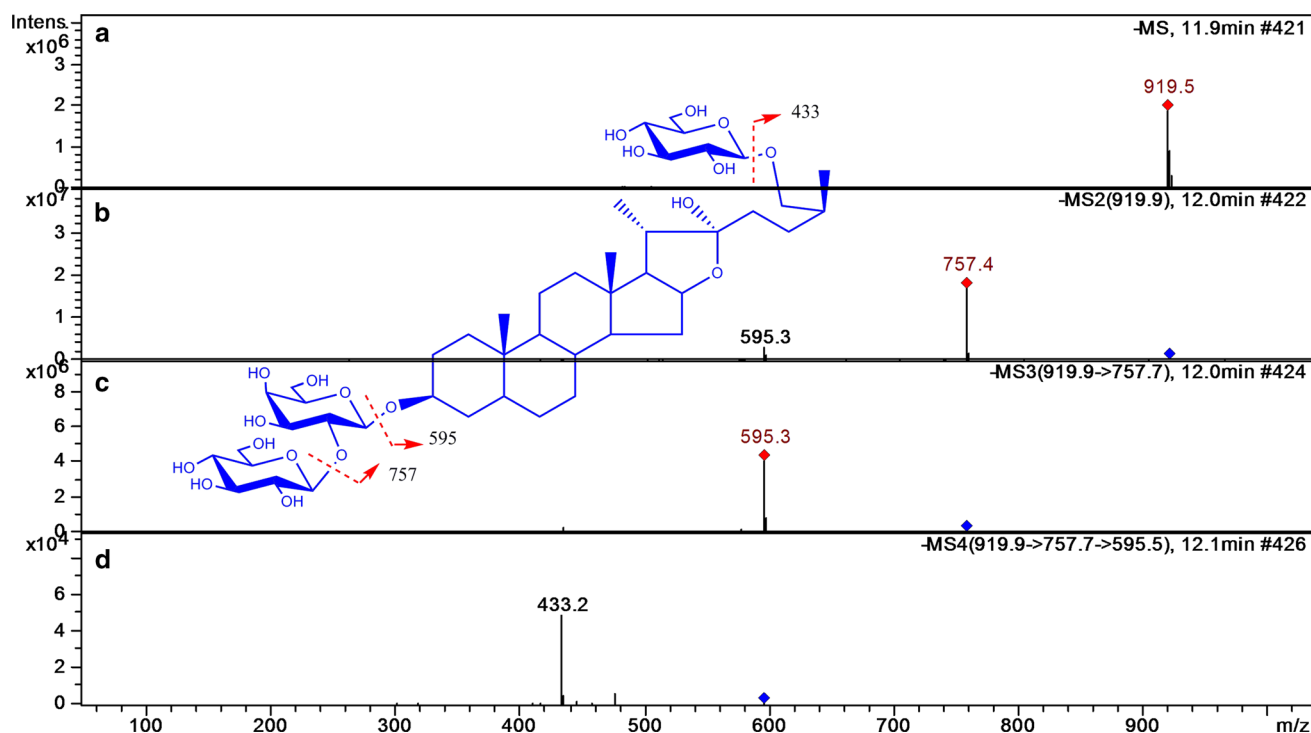
Fig. 5 ESI(-) MS^n spectra of TB-II: **a** MS spectrum of the [M-H]- ion at *m/z* 919; **b** MS^2 spectrum of the ion at *m/z* 919; **c** MS^3 spectrum of the ion at *m/z* 757 from the *m/z* 919 ion; **d** MS^4 spectrum of the ion at *m/z* 595 from the *m/z* 757 ion

their further structural determination required other techniques such as ^{1}H and ^{13}C NMR.

Oxidation Metabolite (M18)

Previously, our group obtained a derivative of TB-II by acid hydrolysis and acetylation and determined its structure by NMR [18]. The metabolites of **M18** possessed the same chromatographic behaviors and mass spectra characters as those of TB-II-d. Thus, **M18** could be identified as TB-II-d, an oxidation metabolite of **M19**.

E-ring Cleavage Metabolites (M14)

M14 ($t_R = 16.5$ min) presented the [M-H]$^-$ ion at *m/z* 639, which was 262 Da less than that of **M1** (TB-III). The product ions at *m/z* 477 and 459 originated from the successive loss of glucose molecules (162 Da) and a neutral H_2O (18 Da). Based on the above data and literature [21, 23], **M14** was tentatively identified as the glycosylated isopregnanolone, formed via the cleavage of the E-ring during the metabolism process.

Distribution of TB-II and its Metabolites   After oral administration, samples of rat heart, liver, spleen, lung, kidney and brain were collected and analyzed by the LC-ESI-MS^n method. According to the results, the tissue distribution of

TB-II and its metabolites showed great differences after oral administration to rats. The parent compound (**M0**) and its metabolites (**M9**) were identified in kidney and heart. **M0** and its seven metabolites (**M4**, **M5**, **M9**, **M10**, **M11**, **M12**, **M12** and **M13**) were screened in liver. No metabolites were observed in rat lung, spleen and brain in this study. The results indicated that liver, heart and kidney were the major distribution organs of TB-II in rats.

As for **M13** ($t_R = 23.7$ min), it gave a [M-H]$^-$ ion at *m/z* 737 and product ions [M-C$_6$H$_{10}$O$_5$-H]$^-$ at *m/z* 575 and [M-2 × C$_6$H$_{10}$O$_5$-H]$^-$ at *m/z* 413, which were all 18 Da less than that of **M10**, **M11** and **M12** (hydroxylated TA-III). Thus, **M13** was tentatively identified as the dehydration metabolite of hydroxylated TA-III, and it was only detected in liver.

Metabolism of TB-II In Vitro

After incubation with AGJ and AIJ, ten compounds (**M0**, **M1**, **M5**, **M7**, **M9–M12**, **M14**, **M17**) were detected in the AGJ incubation samples, while seven metabolites (**M1**, **M9**, **M14–M17**, **M19**) were observed in the AIJ incubation samples. **M15** and **M16** were identified as follows. **M15** ($t_R = 17.6$ min) and **M16** ($t_R = 20.0$ min) showed the same [M-H]- ions at *m/z* 595, revealing that these two compounds were isomers. Moreover, the major product ions at 433 [M-H-Glu]$^-$, 415 [M-H-H_2O-Glu]$^-$ and
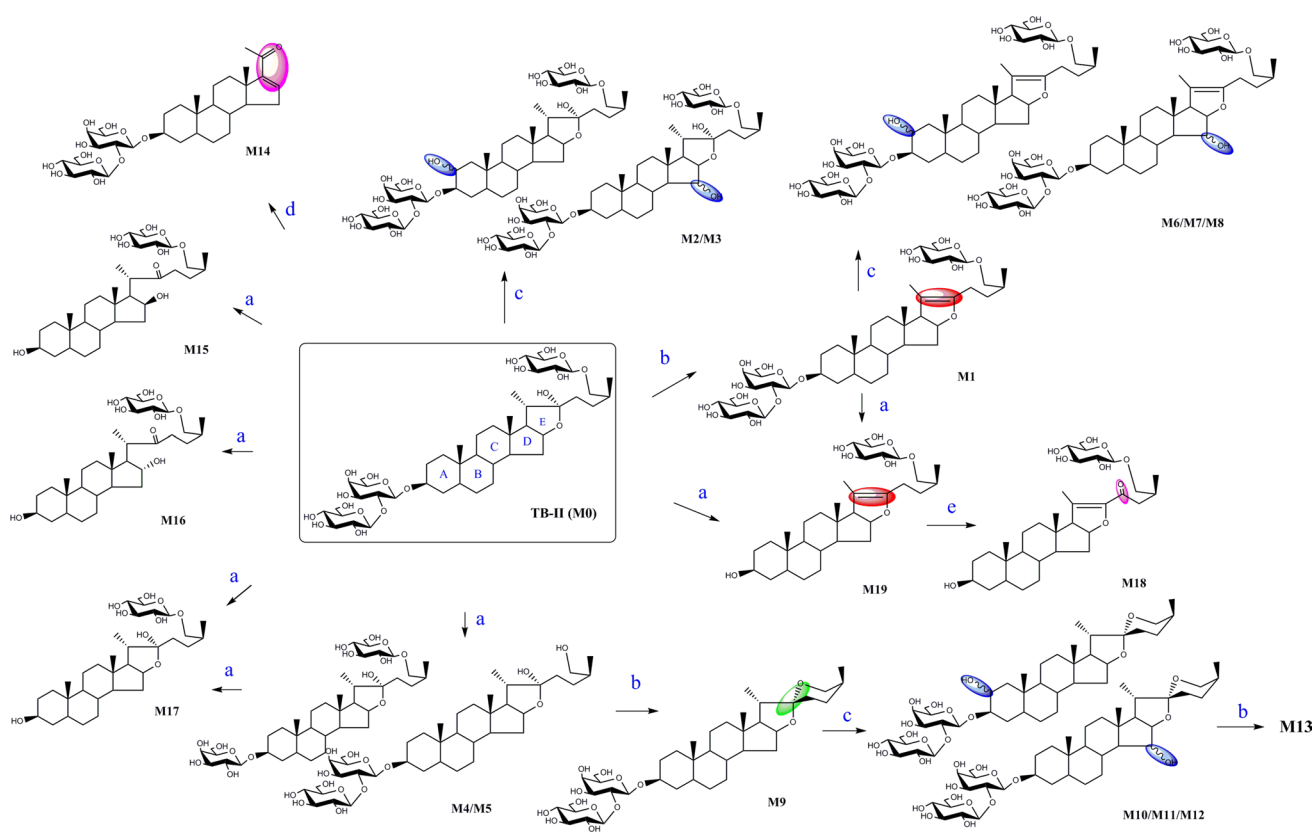
Fig. 6 Structures of TB-II metabolites in rats and possible metabolic pathways for their production: *a* deglycosylation; *b* dehydration; *c* hydroxylation; *d* E-ring cleavage; *e* oxidation

289 [M-H-H$_2$O-Glu-C$_8$H$_{16}$O]$^-$ could be detected in MS^2 and MS^3 spectra. The above fragmentations and retention behavior were consistent with the known TB-III-a and TB-III-c; thus, **M15** and **M16** were unambiguously identified as TB-III-a and TB-III-c, respectively.

Combining these results, we came to the conclusion that the gastrointestinal tract is the major site of TB-II metabolism. The hydrolysis of TB-II was considered an initial step in the biotransformation, allowing for easier diffusion and absorption in the intestines.

Conclusion

The results described in this work illustrated a specific and sensitive HPLC-ESI-MS^n method for the identification of TB-II and its in-vivo and in-vitro metabolites for the first time. Except for **M1**–**M3** and **M9**, all other compounds, especially the five artificial steroidal saponins, were first reported as the metabolites of TB-II. The proposed metabolic pathways of TB-II in rats were thought to be dehydration, deglycosylation, oxidation and E-ring cleavage (shown in Fig. 6). This study provided systematic and valuable information on the in-vivo and in-vitro metabolism of TB-II, which could be the basis for explaining the pharmacological actions of TB-II and used for further application in preclinical studies. The pharmacological activities of its metabolites will be examined in future investigations.

Compliance with ethical standards We confirm that the manuscript has been read and approved by all named authors and that there are no other persons who satisfied the criteria for authorship but are not listed. All authors involved have no commercial association or other arrangement that might pose or imply a conflict of interest in connection with the submitted article. All of the animal care and experimental procedures were approved by the Animal Ethical Committee of Shanghai Institute of Materia Medica (Shanghai, China).

References

1. Nagumo S, Kishi S, Inoue T, Nagai M (1991) Yakugaku Zasshi 111(6):306–310
2. Nakashima N, Kimura I, Kimura M, Matsuura H (1993) J Nat Prod 56(3):345–350
3. Ma CH, Fan MS, Tang YH, Li ZX, Sun ZL, Ye G, Huang CG (2008) Biomed Chromatogr 22:835–850

4. Ma CH, Wang LX, Tang YH, Fan MS, Xiao HB, Huang CG (2008) Biomed Chromatogr 22:1066–1083

5. Lu WQ, Oiu Y, Li TJ, Tao X, Sun LN, Chen WS (2011) Clin Exp Pharmacol P 38:430–434

6. Kang LP, Zhang J, Cong Y, Li B, Xiong CQ, Zhao Y, Tan DW, Yu HS, Yu ZY, Cong YW, Liu C, Ma BP (2012) Planta Med 78:611–616

7. Lu WQ, Oiu Y, Li TJ, Tao X, Sun LN, Chen WS (2009) Arch Pharm Res 32:1301–1308

8. Xiao SZ, Xu ME, Ge YK, Xiao GF (2006) Biomed Environ Sci 19:185–191

9. Li TJ, Qiu Y, Yang PY, Rui YC, Chen WS (2007) Neurosci Lett 421:147–151

10. Deng Y, Ma BP, Cong YW, Shen YX, Zhang JJ, Shen YJ (2009) Chin Pharmacol Bull 25(2):244–247

11. Lu MZ, Zhang ZQ, Yi J, Chen WS, Hou ZH, Li TJ (2010) J Pharm Pract 28:283–287

12. Cai F, Sun LN, Gao SH, Yang Y, Yang Q, Chen WS (2008) J Pharm Biomed Anal 48:1411–1416

13. Cai F, Xu W, Wei H, Sun LN, Gao SH, Yang Q, Feng J, Zhang F, Chen WS (2010) J Chromatogr B 878:1845–1854

14. Liu ZR, Liu M, Qi YP, Zhu ZY, Chai YF, Yuan C, Lin Y (2013) J Sep Sci 36:1659–1666

15. Liu ZR, Dong X, Ding X, Chen XF, Lv L, Li YY, Chai YF (2013) J Chromatogr B 926:28–35

16. Feng Y, Chen BT, Lin AH, Liu YM (2014) J Chromatogr B 965:119–126

17. Wu B, Liu ZY, Fan MS, Sun ZL, Jiang WX, Huang CG (2012) Chin Chem Lett 23:332–334

18. Guo J, Xu CH, Xue R, Jiang WX, Wu B, Huang CG (2014) Arch Pharm Res. doi:10.1007/s12272-014-0431-4

19. Xiao Y, Cao JH, Zhao SW, Jiang DX, Zhang D (2011) West China J Pharm Sci 26(4):389–390

20. Appolpnova SA, Shpak AV, Semenov VA (2004) J Chromatogr B 800:281–289

21. Liu ZR, Zhu DL, Lv L, Li YY, Dong X, Zhu ZY, Chai YF (2012) Rapid Commun Mass Spectrom 26:1955–1964

22. Kang LP, Zhang J, Cong Y, Li B, Xiong CQ, Zhao Y, Tan DW, Yu HS, Yu ZY, Cong YW, Liu C, Ma BP (2012) Planta Med 78:611–616

23. He XJ, Qiao AM, Wang XH, Liu B, Jiang MM, Su LN, Yao XS (2006) Steroids 71:828–833